Design, synthesis and CoMFA studies of N1-amino acid substituted 2,4,5-triphenyl imidazoline derivatives as p53–MDM2 binding inhibitors

Chunqi Hu [a], Xiaoxue Dou [a], Yizhe Wu [a], Lei Zhang [b], Yongzhou Hu [a,*]

[a] ZJU-ENS Joint Laboratory of Medicinal Chemistry, College of Pharmaceutical Sciences, Zhejiang University, Hangzhou 310058, China
[b] Institute of Pharmacology and Toxicology, College of Pharmaceutical Sciences, Zhejiang University, Hangzhou 310058, China

ARTICLE INFO

ABSTRACT

A series of novel N1-amino-acid substituted 2,4,5-triphenyl imidazoline derivatives was designed and synthesized based on our previous studies. All synthesized target compounds were screened for their p53–MDM2 binding inhibitory activities and anti-proliferative activities against five cancer cell lines. Among them, twelve compounds displayed improved binding inhibitory activities and most compounds showed higher cell growth inhibition activities with IC_{50} values in the low micromolar range. Compound **6c** exhibited marked p53–MDM2 binding inhibitory activity ($IC_{50} = 0.59\ \mu M$) which was eightfold more potent than that of Nutlin-1 ($IC_{50} = 4.78\ \mu M$). CoMFA analysis was performed based on obtained biological data and resulted in a statistically significant CoMFA model with high predict abilities ($q^2 = 0.645$, $r^2 = 0.979$).

1. Introduction

The tumor suppressor p53 is a potent transcription factor that controls a major pathway protecting cells from malignant transformation, and plays a pivotal role in blocking tumor genesis and development.[1,2] The p53 tumor suppressor is controlled by the murine double minute 2[3] (MDM2, also frequently referred to as HDM2 in human), which binds to p53 and negatively regulates its transcriptional activity and stability.[4] In unstressed cells, protein levels of p53 are tightly controlled by MDM2 protein through a negative feedback loop.[5] Since more types of cancers are tolerant to elevated levels of wild-type p53,[6] the reactivation of p53 by antagonizing p53–MDM2 interaction offers a new therapeutic strategy for cancer therapy.

Series of compounds have been developed as p53–MDM2-binding inhibitors in recent decades.[6–12] Nultins were the first potent and selective p53–MDM2 interaction inhibitors that were discovered through high throughput screening. And Nutlin-3[9] was one of the most potent molecules of Nutlins that demonstrated promising bioactivities in vitro and in vivo.

In our previous study, three new series of imidazoline derivatives were designed and synthesized using Nultins as lead compounds.[12] The imidazoline scaffold of Nutlins was retained as the core structure with a focus on modifying the phenyl groups on the imidazoline ring and the N-1 side chain of Nutlins. Based on the obtained data, a preliminary SAR was disclosed that the three phenyl groups

were essential for the potency, and the N-1 substituents displayed a very important role in remaining the potencies as well.

Hence, we designed and synthesized a series of novel Nutlin analogs, utilizing amino acids, amino-acid esters or amino-acid amides as the N-1 substituents to discover new p53–MDM2 binding inhibitors with enhanced p53–MDM2 binding inhibitory activities and anti-proliferative potencies. Then CoMFA study[13] which was carried out based on the obtained data helped in understanding the interaction between the ligand and the receptor.

## 2. Results and discussion

2.1. Chemistry

The synthetic routes for the imidazoline derivatives are summarized in Scheme 1. Triphenyl imidazoline **5** was obtained according to previous studies.[12] Then, N-formylation reaction of **5** was performed using bis(trichloromethyl)carbonate in dichloromethane at the presence of triethylamine. The obtained formylchloride was reacted with corresponding amino-acid ethyl esters to give **6a–e**, whose ester groups were further hydrolyzed by 6 N HCl to form acids **7a–e**.[14] Amidation of **7a–e** with secondary amines in the presence of DCC-HOBt gave amides **8a–m**.

2.2. Biological activity

All synthesized compounds were evaluated for their p53–MDM2 binding inhibitory activities by fluorescence-polarization (FP)-based binding assay[14] and anti-proliferation activities by
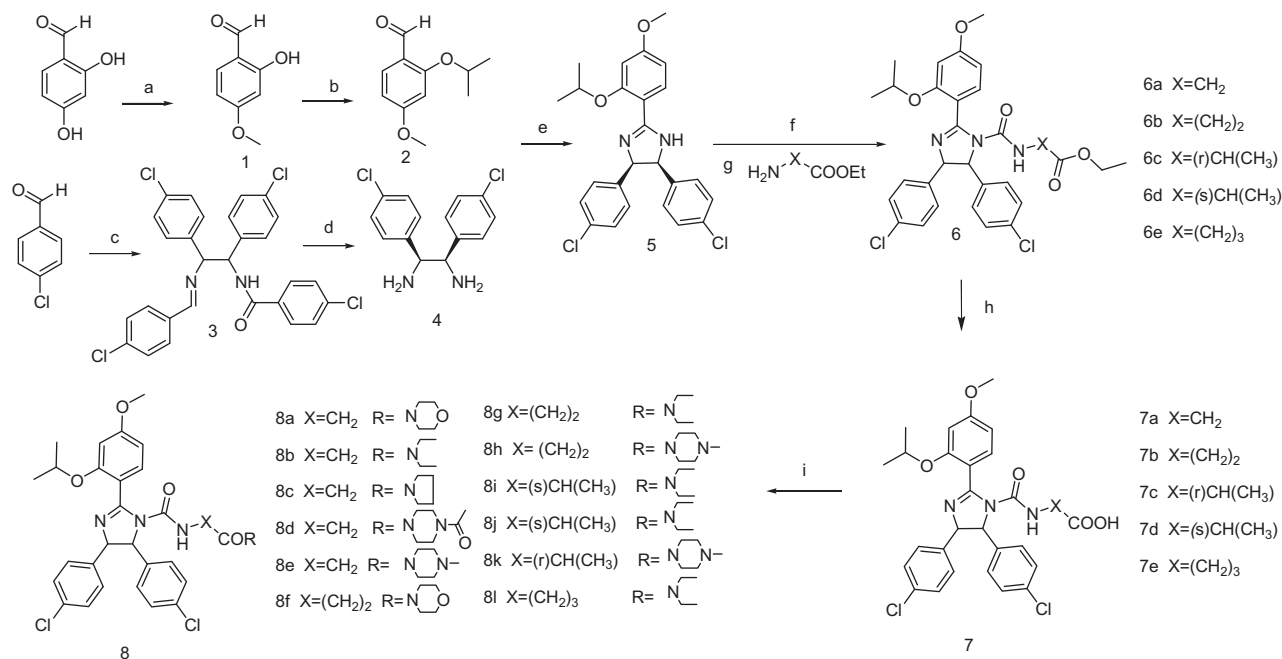
Scheme 1. Reagents and conditions: (a) $(CH_3)_2SO_4$, K_2CO_3, acetone, reflux, 3 h; (b) i-PrBr, K_2CO_3, acetone, 40 °C, 5 h; (c) CH_3COONH_4, reflux, 3 h; (d) H_2SO_4, 120 °C, 3 h; (e) NBS, CH_2Cl_2, rt, 24 h; (f) BTC, CH_2Cl_2, TEA; (g) $H_2NXCOOEt$, TEA, CH_2Cl_2; h.6 N HCl, refluxing, 1 h; (i) RH, HoBt, DCC, CH_2Cl_2.

MTT assay in vitro against five human cancer cell lines including human colon cancer cells HCT116, human lung adenocarcinoma epithelial cells A549, human colon adenocarcinoma SW620 cells, human pancreatic carcinoma cells PC3 and human promyelocytic leukemia cells HL60. Nutlin-1 was employed as the positive control. The results are presented in Table 1.

As shown in Table 1, twelve compounds (**6a–e, 7b–e, 8f–g** and **8l–m**) displayed improved binding inhibitory activities. Compound **6c** exhibited potent inhibitory activity ($IC_{50} = 0.59$ μM), which was almost eightfold better than that of Nutlin-1($IC_{50} = 4.78$ μM). Comparing the various substituents on N-1 revealed that amino-acid esters possessed significant improved binding inhibitory activities, while hydrolyzing esters to corresponding acids reduced inhibitory potencies. When the acids were amidated with amines, the type of amides influenced the binding inhibitory activities obviously. Compounds with a 3-aminopropanamide side chain (i.e., **8f** and **8g**) showed enhanced potencies than molecules with a 2-aminoacetamide (i.e., **8a** and **8b**) or a 2-aminobutanamide (i.e., **8m**) the length of the alkyl linker between the N-1 and amines influenced the binding inhibitory activities obviously. Interestingly, the introduction of D-alanine (**8k–l**) as the linker presented better potency than that of L-alanine (**8i–j**).

For the results of MTT assay, nearly all target molecules exhibited enhanced anti-proliferative activities against five tumor cell lines than that of Nutlin-1, indicating that the introduction of amino acid derivatives as the linkers was beneficial to anti-proliferative activities.

2.3. 3D-QSAR analysis

3D-QSAR methods, such as CoMFA, are widely used in drug design because they allow rapid generation of QSAR models, with which biological activity of newly designed molecules can be predicted.[15] In this study, 30 compounds (including Nutlin-1, 14 obtained molecules in this study and 15 molecules in a previous study[12]) with available IC_{50} values were employed for the 3D-QSAR analysis. For 3D-QSAR analyses, 20 compounds (unasterisked molecules in Table 2) were selected as the training set for model construction, and the remaining 10 compounds (asterisked molecules in Table 2) as the testing set for model validation. The alignment of all compounds used in the training set was given in Figure 1. The pIC_{50} values ($pIC_{50} = -\log IC_{50}$) of these compounds were used as dependent variables. The CoMFA results are summarized in Table 3 and the contour maps of CoMFA model were presented in Figure 2.

The statistical parameters for the CoMFA models were given in Table 3. For the CoMFA model, partial least squares (PLS) regression produced an excellent cross-validated correlation coefficient (q^2) of 0.645 (>0.5) with an optimized component of 5, which suggested that the model was reliable and it should be a useful tool for predicting the IC_{50} values. The noncross-validated PLS analysis gave a high correlation coefficient (r^2) of 0.979, and a low standard error estimate (SEE) of 0.115. The contributions of steric and electrostatic fields to this model were 0.626 and 0.374, respectively. The relationship between actual and predicted pIC_{50} of the training set and test set compounds of the CoMFA model are illustrated in Figure 3. The predictive correlation coefficient (R^2_{pred}) value based on molecules of the training set was 0.982 for the CoMFA model, and 0.802 for the test set. The actual and predicted pIC_{50} values of the training set and test set by the model are given in Table 3. The steric contour plot shown in Figure 2A showed a huge green colored contour near the N-substituent of the imidazoline derivatives, indicating that the bulky substitute near the nitrogen atom of the linker was favorable to potency. In addition, CoMFA electrostatic contour map as shown in Figure 2B showed a big blue contour at the end of N-1 substituent, indicating that more positively charged groups in this region enhanced activity. This model could well explain why the potent activity of compound **6c** was better than **7c**. The ethyl ester was in the green and blue region, removing the ethyl group to acid made it inaccessible to the green and blue region.
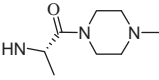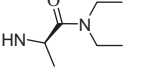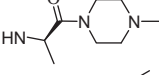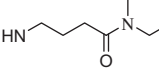
3. Conclusion

Twenty-three N-1 amino acid substituted 2,4,5-triphenyl imidazoline derivatives were designed and synthesized as p53–MDM2 binding inhibitors based on previously discovered

Table 1
p53–MDM2 binding inhibitory and anti-proliferative activities of synthesized compounds (**6a–e**, **7a–e**, and **8a–m**)

	R$_1$	IC$_{50}$-FP[a] (µM)	IC$_{50}$ (µM)				
			HCT116	A549	SW620	PC3	HL60
Nutlin-1		4.87	20.46	24.00	33.72	40.57	19.50
6a		4.29	4.74	3.63	3.88	6.89	2.93
6b		3.36	9.22	14.32	9.41	8.59	7.82
6c		0.59	3.73	0.31	5.52	2.2	3.78
6d		0.84	—[b]	—	—	—	—
6e		1.66	6.65	3.25	8.02	6.2	5.81
7a		6.18	6.07	0.48	5.7	3.9	5.73
7b		1.07	-	-	-	-	-
7c		3.27	5.95	1.67	9.2	5.59	6.7
7d		3.39	—	—	—	—	—
7e		2.05	6.07	0.48	5.7	3.9	5.73
8a		5.27	5.63	10.92	6.25	7.02	2.99
8b		9.41	5.10	4.33	12.35	5.84	6.08
8c		10.35	3.99	3.13	2.90	5.87	6.11
8d		5.43	6.41	3.42	8.13	7.10	5.48
8e		20.65	4.49	3.62	6.17	3.55	3.29
8f		2.23	3.78	3.96	5.89	7.58	3.60
8g		0.65	6.39	4.03	3.13	7.26	4.62
8h		5.83	2.36	5.95	5.99	6.83	2.93
8i		12.62	2.01	3.31	4.60	5.32	4.22

Table 1 (continued)

R$_1$	IC$_{50}$-FP[a] (µM)	IC$_{50}$ (µM)				
		HCT116	A549	SW620	PC3	HL60
8j	12.45	–	–	–	–	–
8k	5.01	7.53	>50	8.56	16.82	8.48
8l	5.96	3.71	2.97	2.74	6.74	3.17
8m	4.18	4.26	1.38	6.45	7.54	6.93

[a] Values are means of three experiments.
[b] NA, no activity.

SARs. In vitro biological evaluation for their p53–MDM2 binding inhibitory activities and anti-proliferative activities revealed that twelve compounds displayed improved binding inhibitory activities and most compounds showed enhanced cell growth inhibition activities. Compound **6c** exhibited marked p53–MDM2 binding inhibitory activity (IC$_{50}$ = 0.59 µM) which was eightfold more potent than that of Nutlin-1 (IC$_{50}$ = 4.78 µM). CoMFA model was performed based on obtained biological data. The CoMFA model was statistically significant with high predictabilities (q^2 = 0.645, r^2 = 0.979) and explained the potent activity of compound **6c**.

4. Experimental sections

4.1. Chemistry

Melting points were determined on a Büchi B-540 apparatus and are uncorrected. ^{1}H NMR spectra were recorded on a Bruker 500 M spectrometer with CDCl$_3$ as solvent. Chemical shifts were reported in values (ppm), relative to internal TMS, and J values were reported in Hertz. Mass spectra were recorded on an Esquire-LC-00075 spectrometer. Reagents and solvents were purchased from common commercial suppliers and were used without further purification. Intermediate **1**–**5** were synthesized using previous reported procedures.[12]

4.1.1. Synthesis of N1-amino acid ester substituted imidazoline derivatives (6a–e): General procedures

Bis(trichloromethyl) carbonate (65.0 mg, 0.34 mmol) in dry methylene chloride (10 mL) was added dropwise to a cooled (0 °C) mixture of compound **5** (60 mg, 0.132 mmol) and triethylamine (0.13 mL) in methylene chloride (10 mL). The mixture was stirred for 30 min and then was evaporated under vacuum. The obtained residue was dissolved in dry methylene chloride (10 mL) and was added dropwise to a solution of the amino-acid ethyl esters (2.56 mmol) in methylene chloride (10 mL). After stirred for 15 min at room temperature, the reaction mixture was worked up with aqueous sodium bicarbonate and extracted with methylene chloride. The organic extracts were washed with water and brine, and dried over Na$_2$SO$_4$. The solvent was evaporated and the residue obtained was purified by chromatography over silica gel by gradient eluent (petroleum ether/ethyl acetate/triethylamine = 3:1:0.01−1:1:0.01) to get compound **6a–e**.

4.1.1.1. Ethyl 2-(4,5-bis(4-chlorophenyl)-2-(2-isopropoxy-4-methoxyphenyl)-4,5-dihydro-1H-imidazole-1-carboxamido)acetate (6a).
White solid (88%); mp: 80–83 °C. ^{1}H NMR (500 MHz, CDCl$_3$) δ = 7.60 (d, J = 8.4, 1H), 7.13 (d, J = 7.9, 2H), 7.05 (dd, J = 19.3, 7.9, 4H), 6.95 (d, J = 7.9, 2H), 6.57 (d, J = 8.4, 1H), 6.52 (s, 1H), 5.63 (m, 2H), 5.24 (s, 1H), 4.70 (m, 1H), 4.10 (q, J = 6.9, 2H), 3.86 (s, 3H), 3.81 (d, J = 4.8, 2H), 1.44 (d, J = 5.9, 3H), 1.26 (d, J = 5.8, 3H), 1.19 (t, J = 7.0, 3H). MS (ESI) m/z = 584 [M+H]$^+$.

4.1.1.2. Ethyl 3-(4,5-bis(4-chlorophenyl)-2-(2-isopropoxy-4-methoxyphenyl)-4,5-dihydro-1H-imidazole-1-carboxamido)propanoate (6b).
White solid (85%); mp: 94–98 °C. ^{1}H NMR (500 MHz, CDCl$_3$) δ = 7.50 (d, J = 8.4, 1H), 7.10 (d, J = 8.3, 2H), 7.02 (m, 4H), 6.93 (d, J = 8.4, 2H), 6.53 (dd, J = 8.4, 2.1, 1H), 6.49 (d, J = 2.1, 1H), 5.52 (m, 3H), 4.67 (m, 1H), 4.10 (q, J = 6.9, 2H), 3.84 (s, 3H), 3.46 (m, 2H), 2.29 (m, 2H), 1.44 (d, J = 5.9, 3H), 1.42 (d, J = 6.0, 3H), 1.29 (d, J = 6.1, 3H). MS (ESI) m/z = 592 [M+H]$^+$.

4.1.1.3. (2R)-ethyl 2-(4,5-bis(4-chlorophenyl)-2-(2-isopropoxy-4-methoxyphenyl)-4,5-dihydro-1H-imidazole-1-carboxamido)propanoate (6c).
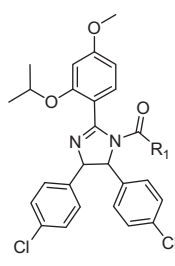White solid (87%); mp: 70–74 °C. ^{1}H NMR (500 MHz, CDCl$_3$) δ 7.60 (d, J = 8.4 Hz, 1H), 7.14–7.02 (m, 7H), 6.96 (d, J = 8.4 Hz, 2H), 6.57 (dd, J = 8.5, 2.2 Hz, 1H), 6.51 (d, J = 2.1 Hz, 1H), 5.08 (s, 4H), 4.74–4.66 (m, 1H), 3.87 (s, 3H), 3.72 (d, J = 7.0 Hz, 1H), 2.34 (td, J = 5.7, 1.5 Hz, 2H), 1.44 (t, J = 5.1 Hz, 3H), 1.32 (d, J = 6.1 Hz, 3H), 1.19 (t, J = 7.1 Hz, 3H). MS (ESI) m/z = 598[M+H]$^+$.
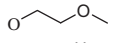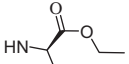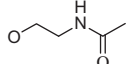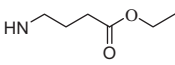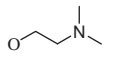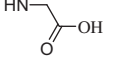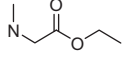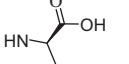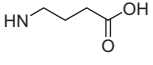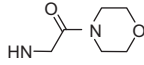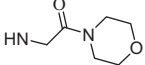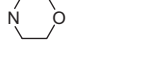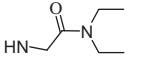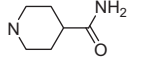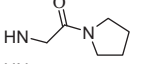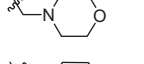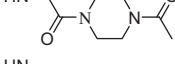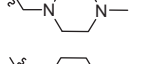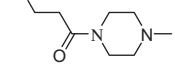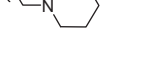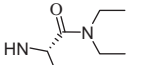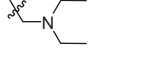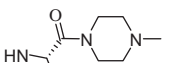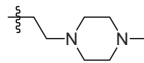
4.1.1.4. (2R)-ethyl 2-(4,5-bis(4-chlorophenyl)-2-(2-isopropoxy-4-methoxyphenyl)-4,5-dihydro-1H-imidazole-1-carboxamido)propanoate (6d).
White solid (78%); mp: 64–48 °C. ^{1}H NMR (400 MHz, CDCl$_3$) δ 7.57 (dd, J = 18.0, 8.4 Hz, 1H), 7.08 (m, 6H), 6.96 (dd, J = 8.4, 1.7 Hz, 2H), 6.55 (m, 2H), 5.61 (m, 2H), 5.03 (d, J = 7.3 Hz, 1H), 4.68 (dt, J = 17.6, 6.0 Hz, 1H), 4.44 (m, 1H), 4.20 (m, 3H), 4.06 (dt, J = 10.8, 5.9 Hz, 2H), 3.85 (m, 3H), 3.27 (m, 1H), 1.37 (m, 3H), 1.29 (m, 3H), 1.15 (dd, J = 5.4, 1.5 Hz, 3H). m/z = 598[M+H]$^+$.

4.1.1.5. Ethyl 4-(4,5-bis(4-chlorophenyl)-2-(2-isopropoxy-4-methoxyphenyl)-4,5-dihydro-1H-imidazole-1-carboxamido)butanoate (6e).
Olily stuff (70%); ^{1}H NMR (500 MHz, CDCl$_3$) δ = 7.55 (d, J = 8.4, 1H), 7.05 (m, 6H), 6.94 (d, J = 8.4, 2H), 6.57 (dd, J = 8.4, 2.2, 1H), 6.53 (d, J = 2.1, 1H), 5.58 (dd, J = 23.4, 10.3, 2H), 4.81 (t, J = 5.5, 1H), 4.70 (dt, J = 12.2, 6.1, 1H), 4.06 (q, J = 7.1, 2H), 3.85 (s, 3H), 3.05 (dd, J = 9.7, 5.8, 2H), 2.09 (dt, J = 7.3, 3.6, 2H), 1.59 (m, 2H), 1.44 (d, J = 6.0, 3H), 1.31 (d, J = 6.1, 3H), 1.21 (t, J = 7.2, 3H). MS (ESI) m/z = 612[M+H]$^+$.

Table 2
Experimental and CoMFA-predicted pIC$_{50}$ values of molecules in both training set and test set

Compds	R$_1$	IC$_{50}$ (µM)	pIC$_{50}$	Predict value	δ	Compds	R$_1$	IC$_{50}$ (µM)	pIC$_{50}$	Predict Value	δ
				5.33	0.02	9a[12]		8.99	5.05	5.08	0.03
6c		0.59	6.23	6.14	−0.09	9b*		2.35	5.63	5.19	−0.44
6e		1.66	5.78	5.69	−0.09	9c		2.24	5.65	5.55	−0.10
7a*		6.18	5.21	4.74	−0.47	9d		6.23	5.21	5.28	0.07
7c		3.27	5.49	5.69	0.20	9e*		13.02	4.89	5.01	0.12
7e*		2.05	5.69	5.72	0.03	9f		1.87	5.73	5.84	0.11
8a		5.72	5.24	5.18	−0.06	9g		15.93	4.80	4.72	−0.08
8b		9.41	5.03	5.02	−0.02	9h		34.34	4.46	4.49	0.03
8c		10.35	4.99	4.98	−0.01	9i*		10.36	4.98	3.66	−1.32
8d*		5.43	5.27	4.69	−0.58	9j		100.89	4.00	3.85	−0.15
8h*		5.83	5.23	4.51	−0.73	9k		321.29	3.49	3.63	0.14
8i		12.62	4.90	4.78	−0.12	9l		399.86	3.40	3.48	0.08
8j		5.96	5.22	5.25	0.03	9m*		3.53	5.45	4.85	−0.60
8k*		5.01	5.30	5.40	0.10	9n		4.77	5.32	5.27	−0.05
8l*		4.18	5.38	5.32	−0.06	9o*		5.10	5.29	5.20	−0.09

4.1.2. Synthesis of N1-amino acid substituted imidazoline derivatives (7a–e): General procedures

A mixture of esters (**6a–e**) and 5 ml 6 N HCl was heated at 110 °C for 1 h. After cooling to room temperature, the reaction mixture was worked up with aqueous sodium bicarbonate and extracted with ethyl ester. The organic extracts were combined, washed with water and brine, and dried over Na$_2$SO$_4$. The solvents were evaporated and the residue was purified by chromatography over silica gel by gradient elution (Dichloromethane/methanol = 9.5:0.5–8:2) to get compounds **7a–e**.

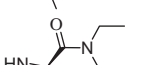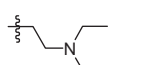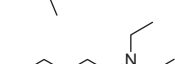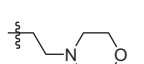#### 4.1.2.1. 2-(4,5-Bis(4-chlorophenyl)-2-(2-isopropoxy-4-methoxyphenyl)-4,5-dihydro-1*H*-imidazole-1-carboxamido)acetic acid (7a).
White solid (52%); mp: 89–92 °C. ^{1}H NMR (500 MHz, CDCl$_3$) δ = 7.61 (d, *J* = 8.4, 1H), 7.17 (d, *J* = 7.9, 2H), 7.04 (m, 3H), 6.95 (d, *J* = 8.1, 2H), 6.53 (d, *J* = 8.4, 1H), 6.48 (s, 1H), 5.57 (t,
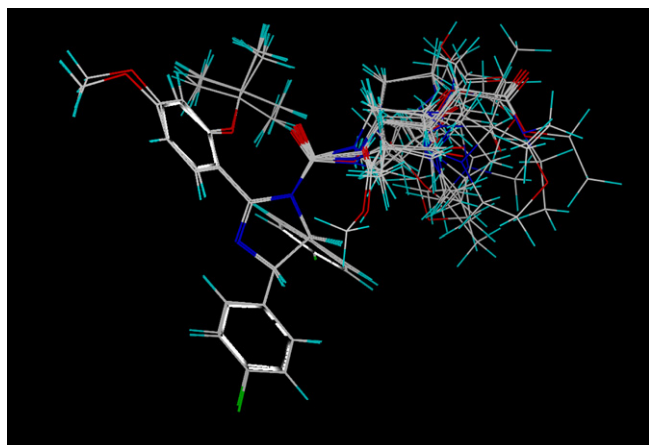
Figure 1. Alignment of all compounds used in the training set.

Table 3
Cross-validated analyses of the CoMFA models using Nutlin-1 as the structural template

Method	SE	Components	q^2	r^2	F	Field contribution	
						Steric	Electrostatic
CoMFA	0.115	5	0.645	0.979	156.259	0.626	0.374

q^2: Leave one out (LOO) cross-validated correlation coefficient.
ONC: optimum number of components.
r^2: non cross-validated correlation coefficient.
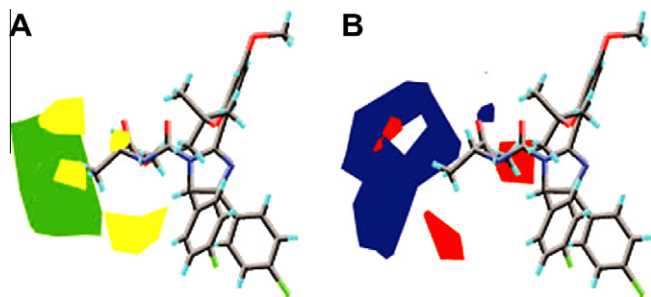SEE: standard error of estimate.
F: F-test value.

Figure 2. CoMFA contour maps for the (A) steric field: Green/yellow contours indicate regions where steric bulky groups increase/decrease activity. Favored and disfavored levels of these displayed fields are fixed at 80% and 20%, respectively. (B) Electrostatic field: Red/blue contours indicate regions where negative charge increase/decrease activity. Favored and disfavored levels of these displayed fields are fixed at 85% and 15%, respectively.

J = 7.9, 2H), 5.47 (s, 1H), 4.67 (m, 1H), 3.83 (s, 3H), 3.64 (dd, J = 9.5, 3.6, 2H), 1.42 (d, J = 5.9, 3H), 1.26 (t, J = 6.3, 3H). MS (ESI) m/z = 556 [M+H]⁺.

4.1.2.2. 3-(4,5-bis(4-chlorophenyl)-2-(2-isopropoxy-4-methoxy-phenyl)-4,5-dihydro-1H-imidazole-1-carboxamido)propanoic acid (7b). White solid (60%); mp: 116–121 °C. ¹H NMR (500 MHz, CDCl₃) δ 7.48 (d, J = 8.4, 1H), 7.10 (d, J = 8.3, 2H), 7.02 (m, 4H), 6.92 (d, J = 8.4, 2H), 6.54 (dd, J = 8.4, 2.1, 1H), 6.50 (d, J = 2.1, 1H), 5.52 (m, 3H), 4.67 (m, 1H), 3.84 (s, 3H), 3.46 (m, 2H), 2.29 (m, 2H), 1.44 (d, J = 5.9, 3H), 1.42 (d, J = 6.0, 3H). MS (ESI) m/z = 570 [M+H]⁺.
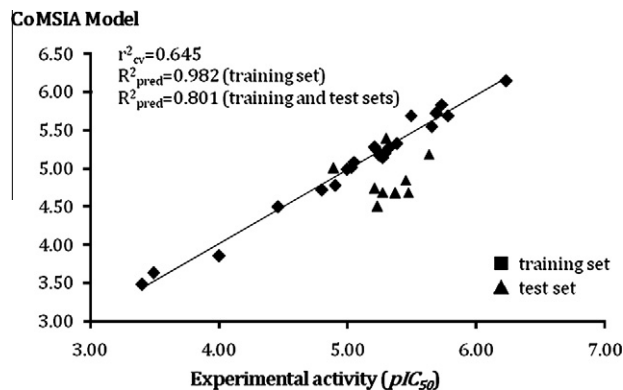

Figure 3. Plot of calculated (predicted) activities versus experimental ones for CoMFA analysis, in which squares indicate values correspond to the 20 compounds in the training set, triangles that of the 10 compounds in the test set.

4.1.2.3. (2R)-2-(4,5-bis(4-chlorophenyl)-2-(2-isopropoxy-4-methoxyphenyl)-4,5-dihydro-1H-imidazole-1-carboxamido)propanoicacid (7c). White solid (45%); mp: 131–134 °C. ¹H NMR (500 MHz, CDCl₃) δ 7.60 (d, J = 8.4 Hz, 1H), 7.14–7.02 (m, 8H), 6.96 (d, J = 8.4 Hz, 2H), 6.57 (dd, J = 8.5, 2.2 Hz, 1H), 6.51 (d, J = 2.1 Hz, 1H), 5.08 (s, 4H), 4.74–4.66 (m, 1H), 3.87 (s, 3H), 3.72 (d, J = 7.0 Hz, 1H), 1.44 (t, J = 5.1 Hz, 3H), 1.32 (d, J = 6.1 Hz, 3H). MS (ESI) m/z = 570[M+H]⁺.

4.1.2.4. (2R)-2-(4,5-bis(4-chlorophenyl)-2-(2-isopropoxy-4-methoxyphenyl)-4,5-dihydro-1H-imidazole-1-carboxamido)propanoic acid (7d). White solid (48%); mp: 135–138 °C. ¹H NMR (500 MHz, CDCl₃) δ 7.60 (d, J = 8.2 Hz, 1H), 7.14–7.04 (m, 8H), 6.96 (d, J = 8.4 Hz, 2H), 6.58 (dd, J = 8.5, 2.2 Hz, 1H), 6.52 (d, J = 2.1 Hz, 1H), 5.09 (s, 4H), 4.74–4.66 (m, 1H), 3.88 (s, 3H), 3.72 (d, J = 7.0 Hz, 1H), 1.44 (t, J = 5.1 Hz, 3H), 1.32 (d, J = 6.1 Hz, 3H). MS (ESI) m/z = 570[M+H]⁺.

4.1.2.5. 4-(4,5-Bis(4-chlorophenyl)-2-(2-isopropoxy-4-methoxy-phenyl)-4,5-dihydro-1H-imidazole-1-carboxamido)butanoic acid (7e). White solid (40%); mp: 101–104 °C. ¹H NMR (500 MHz, CDCl₃) δ = 7.55 (d, J = 8.4, 1H), 7.05 (m, 6H), 6.94 (d, J = 8.4, 2H), 6.57 (dd, J = 8.4, 2.2, 1H), 6.53 (d, J = 2.1, 1H), 5.58 (dd, J = 23.4, 10.3, 2H), 4.81 (t, J = 5.5, 1H), 4.70 (dt, J = 12.2, 6.1, 1H), 4.06 (q, J = 7.1, 2H), 3.85 (s, 3H), 3.05 (dd, J = 9.7, 5.8, 2H), 1.59 (m, 2H), 1.44 (d, J = 6.0, 3H), 1.31 (d, J = 6.1, 3H). MS (ESI) m/z = 584[M+H]⁺.

4.1.3. Synthesis of N1-amide substituted imidazoline derivatives (8a–l): General procedures

Imidazoline acid derivatives (7a–e, 0.40 mM), DCC (151 mg, 0.80 mM) and HOBt (54 mg, 0.40 mM) was dissolved in anhydrous DCM (20 mL) under nitrogen and stirred for 30 min. Then the corresponding amine (0.80 mM) was slowly added with vigorous stirring at rt for about 3 h. The precipitate was filtered; the filtrate was washed with brine, and dried over Na₂SO₄. The solvents were evaporated and the residue was purified by chromatography over silica gel by gradient eluent to get target compounds 8a–l.

4.1.3.1. 4,5-Bis(4-chlorophenyl)-2-(2-isopropoxy-4-methoxy-phenyl)-N-(2-morpholino-2-oxoethyl)-4,5-dihydroimidazole-1-carboxamide (8a). White solid (82%); mp: 80–82 °C. ¹H NMR (500 MHz, CDCl₃) δ 7.62 (d, J = 8.4 Hz, 1H), 7.16 (d, J = 8.3 Hz, 2H), 7.09 (d, J = 8.5 Hz, 2H), 7.04 (d, J = 8.4 Hz, 2H), 6.96 (d, J = 8.4 Hz, 2H), 6.58 (dd, J = 8.5, 2.2 Hz, 1H), 6.52 (d, J = 2.0 Hz, 1H), 5.80 (s, 1H), 5.64 (dd, J = 28.9, 10.3 Hz, 2H), 4.70 (dt, J = 12.2, 6.1 Hz, 1H), 3.92 (dd, J = 17.1, 4.6 Hz, 1H), 3.86 (s, 3H), 3.81 (dd, J = 17.0,

3.7 Hz, 1H), 3.61 (dt, *J* = 9.7, 4.8 Hz, 4H), 3.52 (t, *J* = 7.4 Hz, 2H), 3.31–3.23 (m, 2H), 1.44 (d, *J* = 6.0 Hz, 3H), 1.25 (d, *J* = 6.1 Hz, 3H). MS (ESI) *m/z* = 625 [M+H]⁺.

4.1.3.2. 4,5-Bis(4-chlorophenyl)-*N*-(2-(diethylamino)-2-oxoeth-yl)-2-(2-isopropoxy-4-methoxyphenyl)-4,5-dihydroimidazole-1-carboxamide (8b). White solid (86%); mp: 101–105 °C. ¹H NMR (500 MHz, CDCl₃) *δ* = 7.59 (d, *J* = 8.4, 1H), 7.18 (d, *J* = 8.2, 2H), 7.08 (d, *J* = 8.3, 2H), 7.03 (d, *J* = 8.3, 2H), 6.96 (d, *J* = 8.4, 2H), 6.56 (m, 1H), 6.51 (d, *J* = 1.7, 1H), 5.70 (s, 1H), 5.60 (dd, *J* = 32.3, 10.2, 2H), 4.69 (dt, *J* = 12.1, 6.0, 1H), 3.97 (dd, *J* = 17.0, 4.8, 1H), 3.85 (s, 3H), 3.78 (dd, *J* = 17.0, 3.1, 1H), 3.30 (dt, *J* = 9.5, 7.0, 4H), 1.43 (d, *J* = 6.0, 3H), 1.24 (d, *J* = 6.0, 3H), 1.07 (m, 7H). MS (ESI) *m/z* = 611[M+H]⁺.

4.1.3.3. 4,5-Bis(4-chlorophenyl)-2-(2-isopropoxy-4-methoxy-phenyl)-*N*-(2-oxo-2-(pyrrolidin-1-yl)ethyl)-4,5-dihydroimidaz-ole-1-carboxamide (8c). White solid (70%); mp: 110–115 °C. ¹H NMR (500 MHz, CDCl₃) *δ* = 7.59 (d, *J* = 8.4, 1H), 7.17 (d, *J* = 8.0, 2H), 7.08 (d, *J* = 8.5, 2H), 7.03 (d, *J* = 8.4, 2H), 6.96 (m, 2H), 6.56 (d, *J* = 8.4, 1H), 6.51 (s, 1H), 5.68 (s, 1H), 5.61 (m, 2H), 4.69 (dt, *J* = 12.1, 6.1, 1H), 3.85 (m, 4H), 3.73 (m, 1H), 3.39 (t, *J* = 6.8, 2H), 3.25 (t, *J* = 6.8, 2H), 1.91 (m, 2H), 1.81 (m, 2H), 1.43 (d, *J* = 6.0, 3H), 1.25 (d, *J* = 6.0, 3H). MS (ESI) *m/z* = 623 [M+H]⁺.

4.1.3.4. *N*-(2-(4-acetylpiperazin-1-yl)-2-oxoethyl)-4,5-bis(4-chlorophenyl)-2-(2-isopropoxy-4-methoxyphenyl)-4,5-dihydro-imidazole-1-carboxamide (8d). White solid (73%); mp: 88–90 °C. ¹H NMR (500 MHz, CDCl₃) *δ* = 7.62 (s, 1H), 7.14 (d, *J* = 7.7, 2H), 7.08 (d, *J* = 8.6, 2H), 7.03 (d, *J* = 8.4, 2H), 6.95 (d, *J* = 8.0, 2H), 6.57 (d, *J* = 8.4, 1H), 6.50 (s, 1H), 5.85 (s, 1H), 5.66 (d, *J* = 25.2, 2H), 4.69 (dt, *J* = 12.1, 6.0, 1H), 3.88 (m, 5H), 3.56 (s, 3H), 3.28 (dd, *J* = 14.7, 9.6, 2H), 2.13 (s, 4H), 2.09 (s, 3H), 1.43 (d, *J* = 6.0, 3H), 1.25 (d, *J* = 6.0, 3H). MS (ESI) *m/z* = 666[M+H]⁺.

4.1.3.5. 4,5-Bis(4-chlorophenyl)-2-(2-isopropoxy-4-methoxy-phenyl)-*N*-(3-(4-methylpiperazin-1-yl)-3-oxopropyl)-4,5-dihy-droimidazole-1-carboxamide (8e). White solid (62%); mp: 90–92 °C. ¹H NMR (500 MHz, CDCl₃) *δ* = 7.53 (d, *J* = 8.4, 1H), 7.11 (d, *J* = 8.4, 2H), 7.04 (dd, *J* = 10.2, 8.7, 4H), 6.95 (d, *J* = 8.4, 2H), 6.55 (dd, *J* = 8.4, 2.0, 1H), 6.50 (d, *J* = 1.8, 1H), 5.55 (m, 3H), 4.68 (dt, *J* = 12.1, 6.0, 1H), 3.85 (s, 3H), 3.49 (d, *J* = 4.4, 2H), 3.32 (t, *J* = 5.2, 4H), 2.31 (m, 8H), 1.44 (d, *J* = 6.0, 3H), 1.31 (d, *J* = 6.0, 3H). MS (ESI) *m/z* = 652[M+H]⁺.

4.1.3.6. 4,5-Bis(4-chlorophenyl)-2-(2-isopropoxy-4-methoxy-phenyl)-*N*-(3-morpholino-3-oxopropyl)-4,5-dihydroimidazole-1-carboxamide (8f). White solid (84%); mp: 95–97 °C. ¹H NMR (500 MHz, CDCl₃) *δ* = 7.52 (d, *J* = 8.4, 1H), 7.09 (d, *J* = 8.3, 2H), 7.02 (m, 4H), 6.93 (d, *J* = 8.4, 2H), 6.53 (dd, *J* = 8.4, 2.1, 1H), 6.49 (d, *J* = 2.1, 1H), 5.52 (m, 3H), 4.67 (m, 1H), 3.84 (s, 3H), 3.59 (dd, *J* = 10.9, 5.9, 4H), 3.46 (m, 2H), 3.29 (dd, *J* = 10.5, 5.3, 4H), 2.29 (m, 2H), 1.42 (d, *J* = 6.0, 3H), 1.29 (d, *J* = 6.1, 3H). MS (ESI) *m/z* = 639[M+H]⁺.

4.1.3.7. 4,5-Bis(4-chlorophenyl)-*N*-(3-(diethylamino)-3-oxopro-pyl)-2-(2-isopropoxy-4-methoxyphenyl)-4,5-dihydroimidazole-1-carboxamide (8g). White solid (80%); mp: 71–74 °C. ¹H NMR (500 MHz, CDCl₃) *δ* = 7.55 (d, *J* = 8.4, 1H), 7.12 (d, *J* = 8.3, 2H), 7.05 (dd, *J* = 12.1, 8.5, 5H), 6.96 (d, *J* = 8.4, 2H), 6.54 (m, 2H), 5.55 (dd, *J* = 48.4, 10.3, 3H), 4.69 (dt, *J* = 12.1, 6.1, 1H), 3.26 (m, 6H), 1.44 (d, *J* = 6.0, 3H), 1.31 (d, *J* = 6.0, 3H), 1.06 (m, 6H). MS (ESI) *m/z* = 625 [M+H]⁺.

4.1.3.8. 4,5-Bis(4-chlorophenyl)-2-(2-isopropoxy-4-methoxy-phenyl)-*N*-(2-(4-methylpiperazin-1-yl)-2-oxoethyl)-4,5-dihy-droimidazole-1-carboxamide (8h). White solid (88%); mp:

85–87 °C. ¹H NMR (500 MHz, CDCl₃) *δ* = 7.59 (d, *J* = 8.4, 1H), 7.17 (d, *J* = 8.3, 2H), 7.08 (d, *J* = 8.5, 2H), 7.03 (d, *J* = 8.4, 2H), 6.96 (d, *J* = 8.4, 2H), 6.57 (dd, *J* = 8.4, 2.1, 1H), 6.51 (d, *J* = 2.0, 1H), 5.70 (t, *J* = 3.8, 1H), 5.60 (dd, *J* = 29.4, 10.2, 2H), 4.69 (dt, *J* = 12.1, 6.1, 1H), 3.93 (dd, *J* = 17.1, 4.6, 1H), 3.85 (s, 3H), 3.80 (dd, *J* = 17.1, 3.4, 1H), 3.53 (s, 2H), 3.28 (m, 2H), 2.31 (t, *J* = 4.8, 4H), 2.26 (s, 3H), 1.43 (d, *J* = 6.0, 3H), 1.24 (d, *J* = 6.0, 3H). MS (ESI) *m/z* = 638[M+H]⁺.

4.1.3.9. 4,5-Bis(4-chlorophenyl)-*N*-((*R*)-1-(diethylamino)-1-oxo-propan-2-yl)-2-(2-isopropoxy-4-methoxyphenyl)-4,5-dihydro-imidazole-1-carboxamide (8i). White solid (76%); mp: 76–79 °C. ¹H NMR (500 MHz, CDCl₃) *δ* 7.60 (dd, *J* = 22.4, 8.4 Hz, 1H), 7.19–7.00 (m, 6H), 6.95 (d, *J* = 8.4 Hz, 2H), 6.57 (m, 1H), 6.50 (s, 1H), 5.62 (m, 3H), 4.73–4.63 (m, 1H), 4.63–4.55 (m, 1H), 3.85 (s, 3H), 3.47–3.07 (m, 4H), 1.43 (t, *J* = 5.8 Hz, 3H), 1.27 (t, *J* = 6.0 Hz, 3H), 1.16–0.97 (m, 6H). MS (ESI) *m/z* = 625 [M+H]⁺.

4.1.3.10. (2*R*)-1-(4,5-bis(4-chlorophenyl)-2-(2-isopropoxy-4-methoxyphenyl)-4,5-dihydroimidazol-1-yl)-2-methyl-3-(4-methylpiperazin-1-yl)propane-1,3-dione (8j). White solid (74%); mp: 94–98 °C. ¹H NMR (500 MHz, CDCl₃) *δ* 7.59 (dd, *J* = 37.7, 8.4 Hz, 1H), 7.22–7.13 (m, 3H), 7.12–7.02 (m, 4H), 6.97 (dd, *J* = 8.5, 2.2 Hz, 2H), 6.59 (ddd, *J* = 14.5, 8.4, 2.2 Hz, 1H), 6.53 (d, *J* = 2.1 Hz, 1H), 5.79 (dd, *J* = 50.3, 7.3 Hz, 1H), 5.66 – 5.53 (m, 2H), 4.68 (ddd, *J* = 19.2, 12.7, 6.4 Hz, 2H), 3.87 (d, *J* = 2.2 Hz, 3H), 3.68–3.30 (m, 4H), 2.41–2.30 (m, 5H), 2.28 (s, 3H), 1.45 (dd, *J* = 6.0, 2.6 Hz, 3H), 1.29 (dd, *J* = 10.0, 6.2 Hz, 3H), 1.09 (dd, *J* = 15.9, 6.9 Hz, 3H). MS (ESI) *m/z* = 637[M+H]⁺.

4.1.3.11. 4,5-Bis(4-chlorophenyl)-*N*-((*R*)-1-(diethylamino)-1-oxopropan-2-yl)-2-(2-isopropoxy-4-methoxyphenyl)-4,5-dihy-droimidazole-1-carboxamide (8k). Oilly stuff (68%); ¹H NMR (500 MHz, CDCl₃) *δ* 7.59 (dd, *J* = 22.4, 8.4 Hz, 1H), 7.19–6.99 (m, 6H), 6.95 (d, *J* = 8.4 Hz, 2H), 6.57 (ddd, *J* = 10.8, 8.5, 2.1 Hz, 1H), 6.50 (s, 1H), 5.62 (m, 3H), 4.73–4.63 (m, 1H), 4.63–4.55 (m, 1H), 3.85 (s, 3H), 3.47–3.07 (m, 4H), 1.43 (t, *J* = 5.8 Hz, 3H), 1.27 (t, *J* = 6.0 Hz, 3H), 1.16–0.97 (m, 6H). MS (ESI) *m/z* = 625 [M+H]⁺.

4.1.3.12. 4,5-bis(4-chlorophenyl)-2-(2-isopropoxy-4-methoxy-phenyl)-*N*-((*S*)-1-(4-methylpiperazin-1-yl)-1-oxopropan-2-yl)-4,5-dihydroimidazole-1-carboxamide (8l). White solid (48%); mp: 140–145 °C. ¹H NMR (500 MHz, CDCl₃) *δ* 7.59 (dd, *J* = 22.4, 8.4 Hz, 1H), 7.20–7.00 (m, 6H), 6.95 (d, *J* = 8.4 Hz, 2H), 6.57 (m, 1H), 6.50 (s, 1H), 5.62 (m, 3H), 4.73–4.63 (m, 1H), 4.63–4.55 (m, 1H), 3.85 (s, 3H), 3.47–3.07 (m, 4H), 1.43 (t, *J* = 5.8 Hz, 3H), 1.27 (t, *J* = 6.0 Hz, 3H), 1.16–0.97 (m, 6H). MS (ESI) *m/z* = 625 [M+H]⁺.

4.1.3.13. 4,5-Bis(4-chlorophenyl)-*N*-(4-(diethylamino)-4-oxobu-tyl)-2-(2-isopropoxy-4-methoxyphenyl)-4,5-dihydroimidazole-1-carboxamide (8m). Oilly stuff (88%); ¹H NMR (500 MHz, CDCl₃) *δ* 7.72 (dd, *J* = 5.1, 3.7 Hz, 2H), 7.49 (d, *J* = 8.5 Hz, 1H), 7.45 (dd, *J* = 5.1, 3.8 Hz, 2H), 6.83 (d, *J* = 8.4 Hz, 2H), 6.73 (d, *J* = 8.4 Hz, 2H), 6.42 (d, *J* = 1.8 Hz, 1H), 6.38 (dd, *J* = 8.5, 2.0 Hz, 1H), 5.74 (d, *J* = 10.7 Hz, 1H), 5.69 (s, 1H), 5.59 (d, *J* = 10.7 Hz, 1H), 4.70–4.61 (m, 1H), 4.03 (q, *J* = 7.1 Hz, 2H), 3.79 (d, *J* = 6.8 Hz, 3H), 3.24–3.19 (m, 2H), 3.07 (dd, *J* = 12.9, 6.3 Hz, 2H), 2.35 (t, *J* = 7.0 Hz, 1H), 2.04 (t, *J* = 6.0 Hz, 2H), 1.85–1.78 (m, 1H), 1.61–1.53 (m, 2H), 1.43 (t, *J* = 5.6 Hz, 3H), 1.29 (d, *J* = 6.0 Hz, 3H), 1.25 (t, *J* = 7.1 Hz, 3H), 1.18 (dd, *J* = 12.0, 4.8 Hz, 3H). MS (ESI) *m/z* = 639[M+H]⁺.

4.2. Biological evaluation

4.2.1. MDM2. protein expression and purification

MDM2 (1–118) plasmid was provided by Dr. Shaomeng Wang's group, and transformed into *Escherichia coli* BL-21 (DE3). Cultures

were grown at 37 °C in TB medium, and induced by 0.4 mM IPTG at an OD_{600} of 0.6 at 18 °C for 20 h. Cells were lysed in 50 mM Tries, pH 7.5 buffer containing 500 mM NaCl and 10% glycerol. MDM2 (1–118) was purified from the soluble fraction using Ni–NTA resin, and desalted in PBS buffer pH 7.5, 150 mM NaCl and 10% glycerol. The protein was purified to >95% as judged SDS–PAGE.

4.2.2. Fluorescence polarization competitive binding assay

Measurements were made with an EnVision Multilabel Plate Reader using a 480 nM excitation filter and a 535 nM emission filter. Assays were performed in Corning 384-well black plates. Nutlin-1 was used as the positive control, while DMSO was used as the negative control. Assays were performed in duplicate and repeated at least twice on separate days. Competition experiments were carried out in a total volume of 20 μL 40 mM Tris–HCl, pH 7.5, 150 mM NaCl, and 1 mM DTT, 4% DMSO. Probe peptide was present at a final concentration of 1 nM, and MDM2 was present at a final concentration of 10 μM. Plates were allowed to incubate at room temperature for 1 h prior to measurement.

4.2.3. Cell viability assay

HCT-116, A549, SW620, PC3 and HL60 cells were planted in 96-well plates (4×10^3/well) for 24 h, and subsequently treated with different concentrations of compounds **6a–c, 6e, 7a, c, e**, and **8a–l** for 72 h. Viable cells were determined using MTT assay. MTT solution (5.0 mg/mL in RPIM-1640, Sigma, St. Louis, MO) was added (10.0 μl/well), and plates were incubated for a further 4 h at 37 °C. The purple formazan crystals were dissolved in 100.00 μl DMSO. After the crystal dissolved, the plates were read on an automated microplate spectrophotometer (Bio-Tek Instruments, Winooski, VT) at 570 nm. The concentration for 50% inhibition of cells (IC_{50}) was calculated using the software of Dose-Effect Analysis with Microcomputers.

4.3. 3D-QSAR analysis

4.3.1. Data set and alignment

3D-QSAR studies were performed using SYBYL 6.9 molecular modeling software.[16] All parameters used in CoMFA were default except for explained. Active conformation selection is a key step for 3D-QSAR analyses. Since the crystal structure of complex of MDM2 with one of these compounds is not available, conformation search was performed in Chem3D software to discover the global energy-minimum conformation for the Nutlin-1 by rotating rotatable bonds. The rest of the molecules were built by changing the substitutions of Nutlin-1 and were minimized with the same way. Finally, Gasteiger-Hückel charges were assigned to all molecules.

Structural alignment is considered as one of the most sensitive parameters in CoMFA analysis. The accuracy of the prediction of CoMFA model and reliability of the contour maps are directly dependent on the structural alignment rule. Nutlin-1 was used as

a template for superimposition, and the common fragment with 2,4,5-triphenyl imidazoline scaffold was selected for alignment and all the molecules were aligned on it.

4.3.2. Partial least squares (PLS) analysis and models validation of 3D-QSAR model

Partial least squares (PLS) analysis was used to construct a linear correlation between the 3D-fields and the p53–MDM2 binding inhibitory activities. To select the best model, the cross-validation analysis was performed using the leave-one-out (LOO) method in which one compound was removed from the data set and its activity was predicted using the model built from rest of the data set. It resulted in the cross-validation correlation coefficient (q^2) and the optimum number of components N. The non-cross-validation was performed with a column filter value of 2.0 to speed up the analysis and reduce the noise.

References and notes

1. Levine, A. J. Cell **1997**, 88, 323.
2. Vogelstein, B.; Lane, D.; Levine, A. J. Nature **2000**, 408, 307.
3. Eldeiry, W. S.; Tokino, T.; Velculescu, V. E.; Levy, D. B.; Parsons, R.; Trent, J. M.; Lin, D.; Mercer, W. E.; Kinzler, K. W.; Vogelstein, B. Cell **1993**, 75, 817.
4. Vu, B. T.; Vassilev, L. Small-Mol. Inhib. Protein–Protein Interact. **2011**, 348, 151.
5. Schon, O.; Friedler, A.; Bycroft, M.; Freund, S. M. V.; Fersht, A. R. J. Mol. Biol. **2002**, 323, 491.
6. Bowman, A. L.; Nikolovska-Coleska, Z.; Zhong, H. Z.; Wang, S. M.; Carlson, H. A. J. Am. Chem. Soc. **2007**, 129, 12809.
7. Fischer, P. M.; Lane, D. P. Trends Pharmacol. Sci. **2004**, 25, 343.
8. Issaeva, N.; Bozko, P.; Enge, M.; Protopopova, M.; Verhoef, L. G. G. C.; Masucci, M.; Pramanik, A.; Selivanova, G. Nat. Med. **2004**, 10, 1321.
9. Vassilev, L. T.; Vu, B. T.; Graves, B.; Carvajal, D.; Podlaski, F.; Filipovic, Z.; Kong, N.; Kammlott, U.; Lukacs, C.; Klein, C.; Fotouhi, N.; Liu, E. A. Science **2004**, 303, 844.
10. Hardcastle, I. R.; Ahmed, S. U.; Atkins, H.; Calvert, A. H.; Curtin, N. J.; Farnie, G.; Golding, B. T.; Griffin, R. J.; Guyenne, S.; Hutton, C.; Kallbad, P.; Kemp, S. J.; Kitching, M. S.; Newell, D. R.; Norbedo, S.; Northen, J. S.; Reid, R. J.; Saravanan, K.; Willems, H. M. G.; Lunec, J. Bioorg. Med. Chem. Lett. **2005**, 15, 1515.
11. Parks, D. J.; LaFrance, L. V.; Calvo, R. R.; Milkiewicz, K. L.; Gupta, V.; Lattanze, J.; Ramachandren, K.; Carver, T. E.; Petrella, E. C.; Cummings, M. D.; Maguire, D.; Grasberger, B. L.; Lu, T. B. Bioorg. Med. Chem. Lett. **2005**, 15, 765.
12. Hu, C. Q.; Li, X.; Wang, W. S.; Zhang, L.; Tao, L. L.; Dong, X. W.; Sheng, R.; Yang, B.; Hu, Y. Z. Bioorg. Med. Chem. **2011**, 19, 5454.
13. Liao, S. Y.; Qian, L.; Miao, T. F.; Lu, H. L.; Zheng, K. C. Eur. J. Med. Chem. **2009**, 44, 2822.
14. Seltzer, S. J. Am. Chem. Soc. **1990**, 112, 4477.
15. Cramer, R. D.; Patterson, D. E.; Bunce, J. D. J. Am. Chem. Soc. **1988**, 110, 5959–5967.
16. Yang, S. H.; Van, H. T. M.; Le, T. N.; Khadka, D. B.; Cho, S. H.; Lee, K. T.; Lee, E. S.; Lee, Y. B.; Ahn, C. H.; Cho, W. J. Eur. J. Med. Chem. **2010**, 45, 5493.